JOURNAL OF MATERIALS SCIENCE **39** (2004) 5155–5159

Synthesis of nanocrystalline/quasicrystalline $Mg_{32}(Al,Zn)_{49}$ by melt spinning and mechanical milling

N. K. MUKHOPADHYAY*
Department of Metallurgical Engineering, Banaras Hindu University, Varanasi 221 005, India; Institut für Strukturphysik, TU Dresden, Dresden 01062, Germany
E-mail: mukho@physik.phy.tu-dresden.de

JATIN BHATT
Department of Metallurgical Engineering, Banaras Hindu University, Varanasi 221 005, India; Department of Metallurgical and Materials Engineering, Indian Institute of Technology, Kharagpur, India

A. K. PRAMANICK
MTC Division, National Metallurgical Laboratory, Jamshedpur, India

B. S. MURTY
Department of Metallurgical and Materials Engineering, Indian Institute of Technology, Kharagpur, India

P. PAUFLER
Institut für Strukturphysik, TU Dresden, Dresden 01062, Germany

In the present investigation we have made an attempt to synthesize T-$Mg_{32}(Al,Zn)_{49}$ Frank Kasper phase and investigate the mechanical properties of the T-Phase in micro and nano scale. Single T-Phase (bcc, $a = 1.42$ nm) has been prepared by conventional casting with a proper combination of flux in order to avoid the loss of magnesium from the melt. Chemical analysis by energy dispersive X-ray microanalysis system attached to scanning electron microscope has confirmed the desired composition for T-phase. The as-cast material was then rapidly solidified by melt spinning and mechanically milled using a high-energy ball mill. The samples were characterized by scanning electron microscopy, transmission electron microscopy and X-ray diffraction techniques. The rapidly solidified foils showed the presence of mostly nanoquasicrystalline phases coexisting with a minute amount of crystalline phases in the thin region where the cooling rate is expected to be high. The dark field imaging in electron microscopy clearly confirms the existence of nano phases. Mechanically milled powder exhibited the evolution of nanophases at higher milling time. Microhardness measurement at low load was carried out in both the as-cast and nanophase materials in order to understand the influence of nanophases on the mode of deformation and cracking at low load.

1. Introduction

It is now becoming clear that the size, distribution and volume fraction of fine scale nano-phase can significantly alter the mechanical and physical properties of materials [1, 2]. Following the nanocrystallization route, brittle intermetallics and ceramics can be made to exhibit improved ductility and fracture toughness. Therefore one can design alloys by controlling the microstructure in the nano-scale. A novel way of transforming a material to a metastable state is to reduce its grain size from micrometers to nanometers, when the proportion of atoms at the grain boundaries is equal to or higher than those inside the grains. These nanocrystalline materials have been shown to have properties much improved over those exhibited by conventional grain size (>10 μm) polycrystalline materials. It is the combination of unique compositions and novel microstructures that leads to the extraordinary potential of nanocrystalline materials. The formation of quasicrystals and related approximant crystalline phases is studied in a Mg-Al-Zn alloy system by applying rapid solidification processing (RSP) and mechanical

*Author to whom all correspondence should be addressed (On leave from Banaras Hindu University).

milling (MM) techniques. The crystal structure of $Mg_{32}(Al,Zn)_{49}$ phase has been shown by Bergman *et al*. [3] to be bcc with $a = 1.416$ nm and 162 atoms and contain icosahedral clusters and is a typical Frank-Kasper phase. It has been shown by Ramachandra Rao and Sastry [4] that by rapid solidification this phase can give rise to a quasicrystalline (QC) phase, which is also known as icosahedral phase [5].

In the present investigation we have adopted two processing techniques in order to synthesize nanophase materials. We have produced nanocrystalline and nanoquasicrystalline (nanoQC) phases by RSP from an as-cast Frank-Kasper phase $Mg_{32}(Al,Zn)_{49}$ alloy as well as by MM of the as-cast alloy for up to 60 h in a high energy ball mill. The results obtained in all the cases are discussed in the light of our current understanding.

2. Experimental details

$Mg_{32}(Al,Zn)_{49}$alloy was prepared in a graphite coated fire clay crucible inside a muffle furnace using a protective (high fluidity) flux ($MgCl_2$ + KCl in ratio of 2:3). Melt spinning was used to produce foils of $Mg_{32}(Al,Zn)_{49}$. High energy ball milling using a Pulverisette-P5 planetary ball mill was used to produce fine powder of $Mg_{32}(Al,Zn)_{49}$ alloy. Fine powder was prepared from alloy ingots by ball milling for up to 60 h to study the phase transformation. Milling was done in tungsten carbide vial containing 50 tungsten carbide (WC) balls of 10 mm diameter using a ball-to-powder ratio of 15:1. The rotation speed has been at 300 rpm for this planetary ball mill. The milling was carried out using toluene as a medium to prevent oxidation during milling. For structural characterization the X-ray diffraction (XRD) was carried out by Rigaku X-Ray diffractometer using Cu K_α radiation ($\lambda = 1.5409$ Å) and Phillips PW 1710 using Co K_α radiation ($\lambda = 1.789$ Å). Scanning Electron Microscopy (SEM) was done using a JEOL 840 A having an energy dispersive X-ray (EDX) attachment. Transmission Electron Microscopy (TEM) was done by using a JEOL 200CX operated at 100 kV. We analyzed the full width at half maximum (FWHM) of the Bragg peaks as a function of the diffraction angle. It is known that peak broadening will be due to grain size refinement, induced strain and instrument broadening. Instrumental broadening was determined by calibration with a standard silicon sample and it was considered while calculating the strain and size effect. It is known that the X-ray peak broadening due to small crystallite size is inversely proportional to $\cos\theta$, but due to lattice strain it is proportional to $\tan\theta$. Thus, when $\beta\cos\theta$ is plotted against $\sin\theta$, a straight line is obtained with slope as ε and intercept as $0.9\ \lambda/d$. From these, we have calculated the crystallite size d and lattice strain ε [6]. A Tukon Microhardness tester was used to measure the microhardness of as cast and rapidly solidified sample. Each hardness value reported is typically the average of ten values. The same experiment was conducted with various loads of 5, 10, 25 and 50 g.

3. Results and discussions

3.1. As-cast Mg_{32} $(Al,Zn)_{49}$ Frank-Kasper phase

From the EDX analysis it is confirmed that chemical composition is within the single T-Frank-Kasper phase region of the ternary phase diagram of Mg-Al-Zn alloy [7]. XRD analysis confirmed the bcc structure with lattice parameter $a = 1.42$ nm (Fig. 1a). The XRD trace shows intense peaks at (530), (532), (541) and (710) reflections. Among these (530) and (532) are intimately related to vertex vector (211111) and edge vector (221001) reflections of quasicrystals (following the Elser's indexing scheme for QC phase). It has been shown that the (600) and (532) reflections together form all (221001) type vectors of the icosahedral phase. As a result the (600) reflections and (532) reflections merge together and get more intense than the (530) reflection. It must be emphasized that though all these reflections

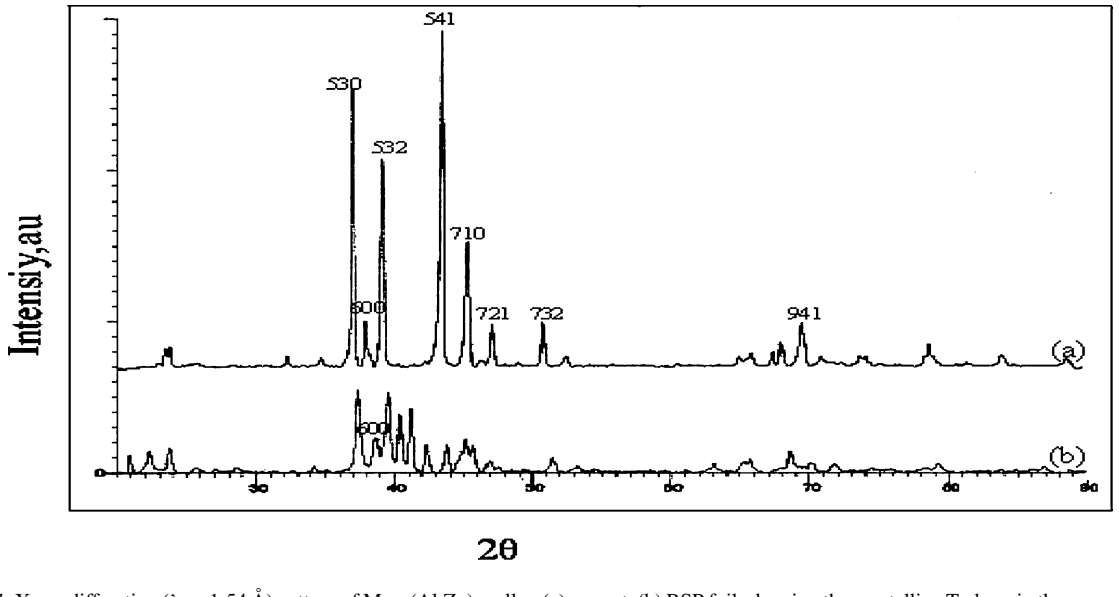

Figure 1 X-ray diffraction ($\lambda = 1.54$ Å) pattern of $Mg_{32}(Al,Zn)_{49}$ alloy (a) as-cast, (b) RSP foil, showing the crystalline T-phase in the as-cast sample and the mixture of QC and T-phases in the RSP foils.

are related to the quasicrystal reflections, there is a shift in all these vectors [8] as has also been seen in the Mg-Al-Ag T-phase [9]. Generally, the peak at (530) is more intense than the peak at (532) in the crystalline phase whereas the reverse is true in the QC phase. The peaks positioned at (530), (532) and (600) reflections are taken as reference peaks to understand the transformation behavior from crystalline to QC phases and vice versa.

3.2. Rapidly solidified $Mg_{32}(Al,Zn)_{49}$ alloy

In the present study RSP foil was made by melt spinning. Diffraction pattern of RSP foil revealed the presence of original bcc along with QC peaks (Fig. 1b). Comparing the peak positions with that of the as-cast structure, the peak shift and the intensity reversal has been observed. This lends support to the fact that the RSP foils contain both quasicrystal and crystalline phases. In RSP foil the peak corresponding to (532) is stronger than (530). This is the basic signature for the formation of QC phase by rapid solidification [9]. Though the crystalline phase of the as-cast alloy has not been completely transformed to the QC phase, however it has changed to a nanostructured phase. TEM analysis of the RSP foils shows a spotty ring diffraction pattern (Fig. 2a) where intense and medium intense rings corresponding to (211 111) and (221 001) reflections of icosahedral quasicrystallline phase (Fig. 2a) were observed. A dark field image (Fig. 2b) obtained from a portion of these two rings shows clearly the presence of the nanostructured phases with particle size ranging from 30 to 50 nm. The formation of nanoQC and nanocrystalline phases, from the as-cast microcrystalline materials is possible because of the high undercooling available during rapid solidification. It can easily be understood that the undercooling required is higher for the formation of nanoQC phase than that of the nanocrystalline phase. It has been shown earlier that a nanoQC phase can be formed in Mg-Al-Zn-Cu system by a gun quenching technique where high undercooling can be attained due to the high cooling rate [10].

3.3. Mechanical milling of as-cast $Mg_{32}(Al,Zn)_{49}$ alloy

In the present study $Mg_{32}(Al,Zn)_{49}$ alloy was milled up to 60 h. Samples were taken after 5, 10, 20, 30, 40, 50 and 60 h of milling for characterization. In as-cast condition (Fig. 1a) the X-ray diffraction pattern revealed the bcc structure of Frank-Kasper phase. After 5 h of milling the XRD pattern (Fig. 3) revealed a decrease in the (600) reflection and an intensification of the (532) reflection, which is a clear indication of the formation of a QC phase. On further milling to 10 h, the (600) peak had completely vanished and the relative intensity of (532) is more than (530) (Fig. 3). On further milling to 20, 30 and 40 h the XRD patterns show a consistent increase in the relative intensity of (532) peak (Fig. 3). As the milling time is increased the peak broadening is seen due to refinement of grain size and induced strain (Fig. 4). The crystallite size

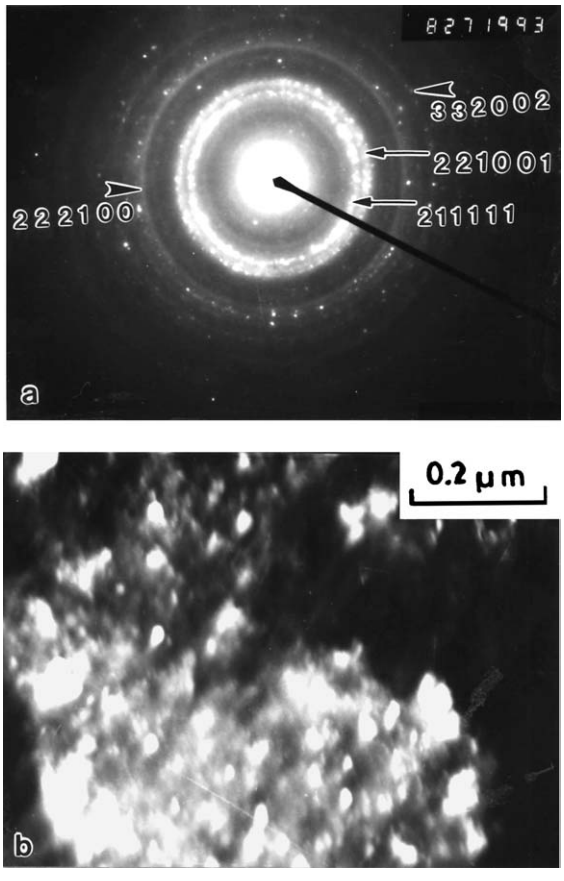

Figure 2 (a) TEM diffraction of RSP foil; (b) Corresponding dark field image using the portion of the intense rings. The rings are indexed in (a) as due to QC phase and the nanoQC phase can be observed from the dark field image in (b).

decreased from 29 to 7 nm and the strain increased from 0.4% to 1.1% as milling time increased from 5 to 60 h. It appears that nanocrystallization has induced a phase transition from crystalline to nanoQC phase. Similar phase transitions in nanocrystalline state have been observed earlier in a number of systems [11]. It is interesting to point out that Bokhonov *et al*. [12, 13] have suggested that icosahedral phase can nucleate topotactically owing to the generation of rotation defects and disorder of lattice plane due to plastic deformation during milling. However during subsequent heat treatment this nanoQC phases transforms back to crystalline Frank-Kasper phase, which is in conformity with the earlier report by Ivanov *et al*. [14].

3.4. Comparison between the results of as-cast and rapidly solidified $Mg_{32}(Al,Zn)_{49}$

Microhardness tests were conducted on both as-cast as well as RSP foil at loads ranging from 5 to 50 g. The microhardness measurement was also carried out at 100 g load for as-cast microcrystalline material where individual crystals of size 10–20 μm are present. The same load could not be applied to the RSP foils due to the thickness of the foil. Therefore, the hardness values of as-cast material as well as RSP foils were compared up to the load of 50 g. Fig. 5 shows the variation of hardness with load in both the as-cast material and RSP foils. The variation of hardness with load (which is

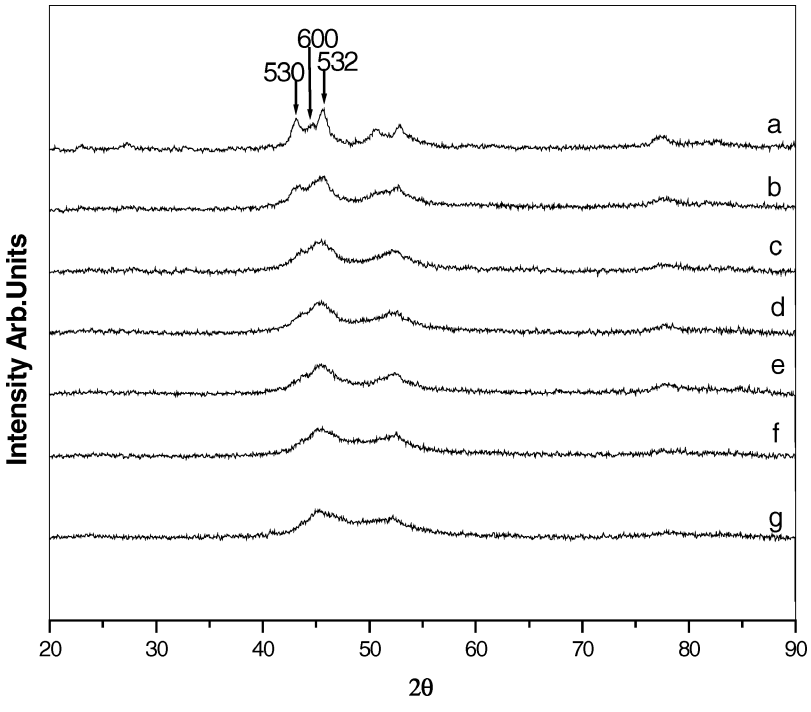

Figure 3 X-ray diffraction ($\lambda = 1.79$ Å) patterns of mechanically milled $Mg_{32}(Al,Zn)_{49}$ powder: (a) 5, (b) 10, (c) 20, (d) 30, (e) 40, (f) 50, (g) 60 h of milling. The important reflections are indicated. It shows the continuous transformation from crystalline to nanoQC phases. The minimum size was found to be ∼7 nm at 60 h of milling.

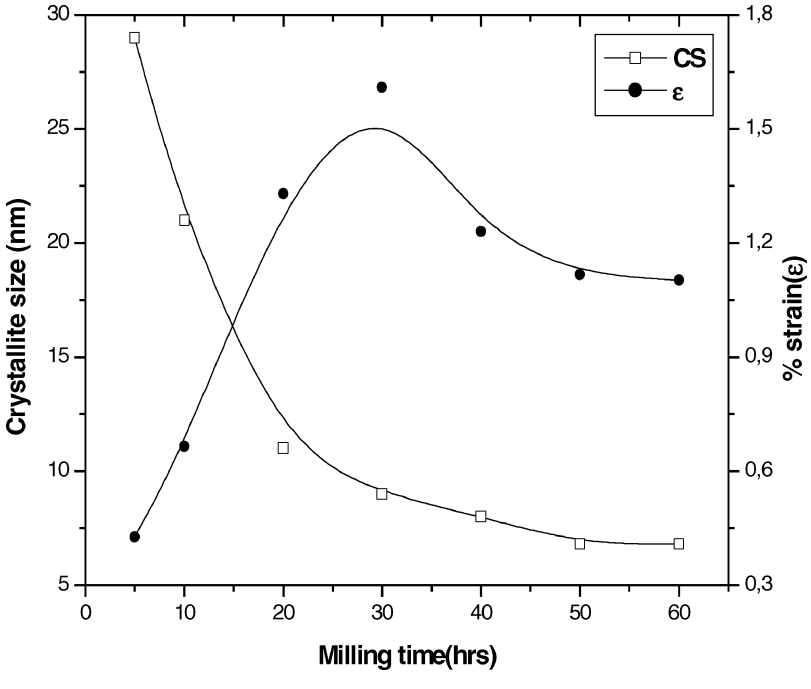

Figure 4 A variation of crystallite size (CS) and strain (ε) with milling time. Two stages of changes in both the curves can be discerned.

known as indentation size effect) is more in case of RSP foils. It has been observed that the cumulative crack length (radial as well as corner) is higher in the case of as-cast material compared to that in the RSP foil, which suggests as-cast is more brittle than the RSP foil. The lengths of this cracks were measured to get the value of fracture toughness, K_{IC}. The relation between K_{IC} and indentation crack length is given by [15], which is expressed as:

$$K_{IC} = 0.035\left(\frac{a}{\sqrt{l}}\right)\left(\frac{H}{E}\right)^{-0.4}\phi^{-0.6}H \qquad (1)$$

where, a = half of indentation diagonal (μm), l = crack length in (μm), H = bulk hardness (GPa); $\phi = H/\sigma_y \approx 3$; E = Young's modulus (GPa); E is taken as 90 GPa for $Mg_{32}(Al,Zn)_{49}$ considering the melting point of the phase. Thus putting all the above values for 50 g load gives

K_{IC} (as-cast) = 0.55 MPa $\sqrt{m}$ where ($a = 8.6$ μm, $l = 11.05$ μm) and

K_{IC} (RSP foil) = 0.924 MPa $\sqrt{m}$ where ($a = 7.24$ μm, $l = 4.25$ μm).

From the above calculation it can be seen that the fracture toughness of the RSP foil containing the

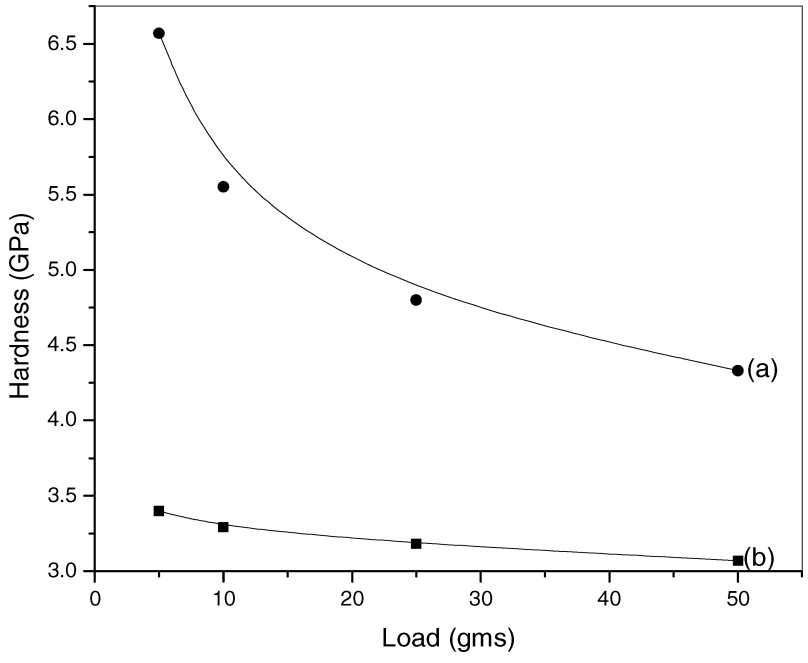

Figure 5 A plot showing microhardness varying with load in $Mg_{32}(Al,Zn)_{49}$ (a) RSP foil (b) as-cast. The variation of the hardness with the load (Indentation Size Effect) can be noticed to be more in RSP foils.

nanophases is nearly twice that of the as-cast sample containing the micro-phases. It is known that the deformation of nanophases is not controlled by dislocation movement, rather it is controlled by grain boundary sliding. The toughness will not be affected significantly whether it is nanoQC or nanocrystalline as in both the cases the same mechanisms are expected to operate. The increase in hardness in the RSP foil may be due to refinement in grain size. Also it is important to notice that the indentation size effect is more pronounced in the nanophase RSP sample than in the microphase as-cast sample. The indentation size effect can be related mostly to the elastic recovery (H/E) [16]. This indicates that the elastic recovery is higher in case of the nanophase material.

4. Conclusions

(1) In RSP foil the nanophases in the order of 30–50 nm are found to consist of nanoQC as well as nanocrystalline phases. It implies that the region where the cooling rate was very fast favored the formation of nanoQC and the region where cooling rate was slow, favored the formation of nanocrystalline phases.

(2) Mechanical milling up to 60 h showed the presence of a dominant nanoQC phase. The average crystallite size obtained in case of the RSP foil was more than 30 nm while in case of 60 h MM it was 7 nm.

(3) Microhardness is greater in case of the RSP foil compared to as-cast $Mg_{32}(Al,Zn)_{49}$, which suggests that the grain refinement has caused the increase of hardness. The fracture toughness of the nanophase sample is nearly twice that of microphase as-cast sample, indicating that the nancrystallites had improved the hardness and toughness of the brittle Frank Kasper phase. It is also observed that the elastic recovery is higher in case of the nanophase RSP material compared to microphase as-cast material.

Acknowledgement

Authors would like to thank Prof. S. Lele, Prof. G. V. S. Sastry and Dr. R. K. Mandal for many stimulating discussions. One of the authors (NKM) acknowledges the support of Alexander von Humboldt Foundation, Germany, for the Research Fellowship during which a part of the work could be completed.

References

1. C. SURYANARAYANA, *Progr. Mater. Sci.* **46** (2001) 1.
2. B. S. MURTY and S. RANGANATHAN, *Int. Mater. Rev.* **43** (1998) 101.
3. G. BERGMAN, J. L. T. WAUGH and L. PAULING, *Acta. Crystal.* **10** (1957) 254.
4. P. RAMACHANDRARAO and G. V. S. SASTRY, *Pramana* **25** (1985) L225.
5. D. SHECHTMAN, I. BLECH, D. GRATIAS and J. W. CAHN, *Phys. Rev. Lett.* **53** (1984) 951.
6. C. SURYANARAYANA, *Progr. Mater. Sci.* **46** (2001) 41.
7. U. MIZUTANI, T. TAKEUCHI and T. FUKUNAGA, *Mater. Trans.* **34** (1993) 108.
8. N. K. MUKHOPADHYAY, K. N. ISHIHARA, K. CHATTOPADHYAY and S. RANGANATHAN, *Acta Metall. Mater.* **39** (1991) 1151.
9. N. K. MUKHOPADHYAY, K. CHATTOPADHYAY and S. RANGANATHAN, *Metall. Trans.* A **20** (1989) 805.
10. N. K. MUKHOPADHYAY, G. N. SUBBANNA, K. CHATTOPADHYAY and S. RANGANTHAN, *Scripta Metall.* **20** (1986) 526.
11. R. Z. VALIEV, R. K. ISLAMGALIEV and I. V. ALEXANDROV, *Progr. Mater. Sci.* **45** (2000) 103.
12. B. BOKHONOV, I. KONSTANCHUNK, E. IVANOV and V. BOLDYREV, *J. Alloys Compd.* **187** (1992) 207.
13. B. BOKHONOV, I. KONSTANCHUNK and V. BOLDYREV, *J. Non-Cryst. Solids* **153/154** (1993) 606.
14. E. YU. IVANOV, I. G. KONSTANCUK, B. B. BOKHONOV and V. V. BOLDYREV, *Reactivity of Solids* **7** (1987) 167.
15. K. NIHARA, *J. Mater. Sci.* **2** (1983) 221.
16. N. K. MUKHOPADHYAY, G. C. WEATHERLY and J. D. EMBURY, *Mater. Sci. Eng.* A **35** (2001) 202.

Received 11 September 2003
and accepted 27 February 2004